

Taking Advantage of Disorder: Small-Molecule Organic Glasses for Radiation Detection and Particle Discrimination

Joseph S. Carlson, Peter Marleau, Ryan A. Zarkesh, Patrick L. Feng

Sandia National Laboratories, 7011 East Ave., Livermore, CA 94550

SUPPORTING INFORMATION

TABLE OF CONTENTS

General Experimental Procedures.....	S3
General Procedure for the Casting of Glasses.....	S4
Synthesis of Compounds 1 – 3	S5
Photoluminescence Spectra for glasses G1 – G6	S7
Characterization of Radioluminescence.....	S10
Radioluminescence Characterization Figures.....	S13
DSC Spectra.....	S16
NMR Spectra.....	S20
Powder X-ray Diffraction Experimental.....	S21
References.....	S21

General Experimental Protocols

All reactions were performed in oven-dried (110 °C) or flame-dried glassware under an atmosphere of dry argon unless otherwise noted. Reaction solvent tetrahydrofuran (THF) was dried by percolation through a column packed with neutral alumina and a column packed with Q5 reactant, a supported copper catalyst for scavenging oxygen, under a positive pressure of argon. Column chromatography was performed using 60 Å (0.040–0.060 mm) mesh silica gel (SiO₂) on a Teledyne ISCO combiflash. 9,10-Diphenylanthracene was recrystallized from xylenes. Iridium (III) bis(2-(4,6-difluorephenyl)pyridinato-N,C2')picolinate (American Dye Source, 90%), 1,4-Bis(2-methylstyryl)benzene (MSB) (Aldrich, Scintillation Grade >99%), 1,4-Bis(5-phenyl-2-oxazolyl)benzene (POPOP) (Aldrich, Scintillation Grade), 4,4'-Bis(2,2-diphenylvinyl)-1,1'-biphenyl (DPVBi) (TCI America, >98%), 2-bromo-9,9-dimethylfluorene (Alfa Aesar, 98%), *n*-butyllithium (2.5M in hexanes), dichlorodiphenylsilane (Aldrich, 97%), and trimethoxyphenylsilane (Aldrich, 97%) were used as received without further purification. ¹H and ¹³C spectra were referenced to residual solvent (CDCl₃: 7.26 ppm, ¹H, 77.16 ppm, ¹³C; C₆D₆: 7.16 ppm, ¹H, 128.06 ppm, ¹³C). Chemical shifts are reported in parts per million, and multiplicities are indicated by s (singlet), d (doublet), t (triplet), q (quartet), quin (quintet), sex (sextet), m (multiplet), br (broad), and app (apparent). Coupling constants, *J*, are reported in Hertz. Mass spectra data are reported in the form of (*m/z*). Visualization of analytical thin-layer chromatography was accomplished with UV (254) and potassium permanganate (KMnO₄) staining solutions. NMR measurements were taken on a Varian 500 MHz spectrometer. Photoluminescence steady state, timing and quantum yield measurements were taken on a Horiba Fluorolog 3-21 spectrometer. For fluorescence

measurements *trans*-stilbene was synthesized via Grubbs metathesis from styrene according to a known procedure.¹ EJ-301 was degassed with argon immediately before use.

General Procedure for the Casting of Glasses

Glass samples were prepared by charging a 5 mL or 20 mL vial with 200 mg or 2.0 g (respectively) of a mixture of **1** and **2** with any desired wavelength shifter. A representative example for a 90:10 ratio of **1** : **2** containing 0.05% (w/w) MSB would contain 1.8 g **1**, 200 mg **2**, and 1 mg of MSB added neat or as a solution in toluene. The vial was placed under high vacuum (<100 mmHg) and brought to the melting point by the application of a heat gun and swirled until completely homogenous. Vacuum was broken to the atmosphere and the liquid was poured into a two-piece aluminum mold (pictured). After allowing the sample to cool (5 min for 200 mg, 20 min for 2.0 gram), the mold was separated from the sample. NOTE: It is important to let the sample cool undisturbed. It has been found that jostling or premature opening of the mold leads to internal stress that can cause the sample to spontaneously fracture. Internal stress can be observed by placing a sample on a light table in between two linear polarizing filters. NOTE: For glass samples containing Flrpic triplet wavelength shifter, the sample is flushed with nitrogen before melting.

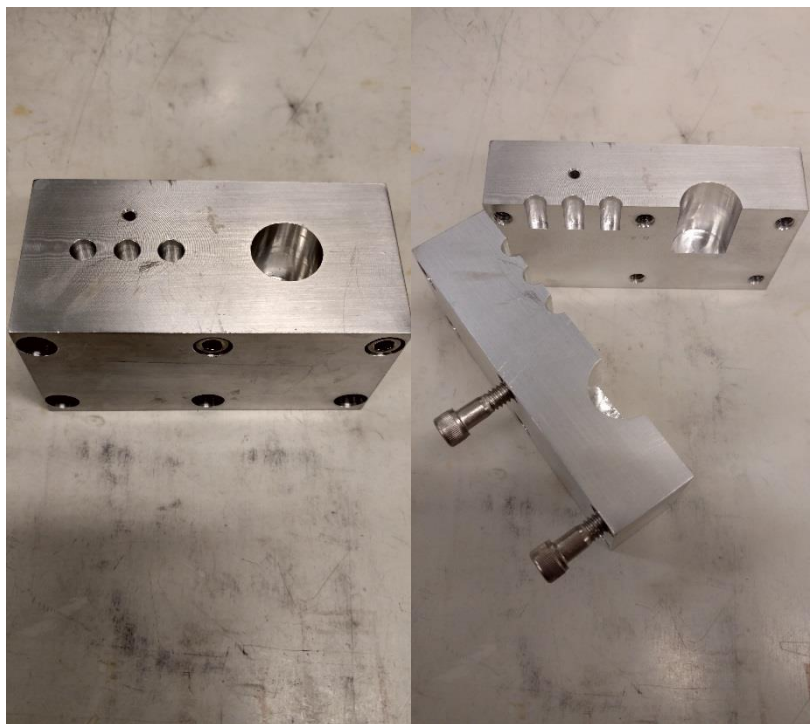
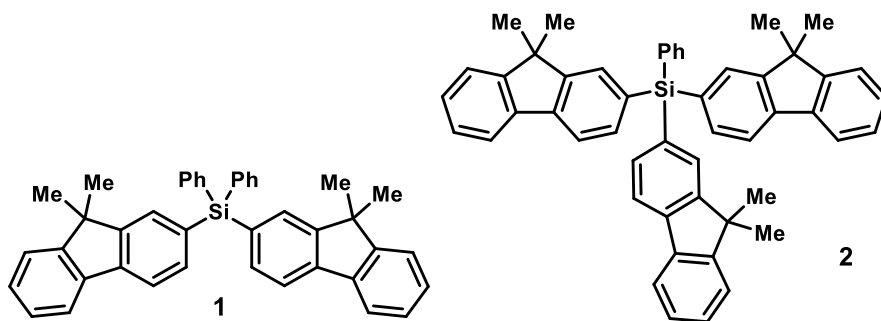
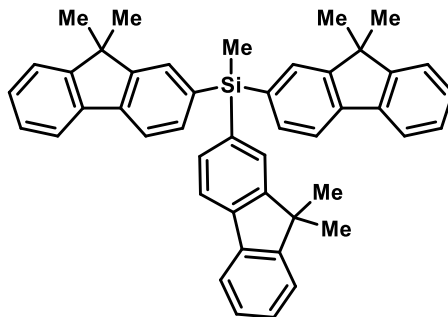


Figure S1. Aluminum mold used to cast organic glasses. Three small $\frac{1}{4}$ " holes for 200 mg samples and $\frac{3}{4}$ " hole for 2 gram samples.

Synthesis of Compounds 1 – 3



Compounds 1 and 2 were synthesized according to literature precedent.²



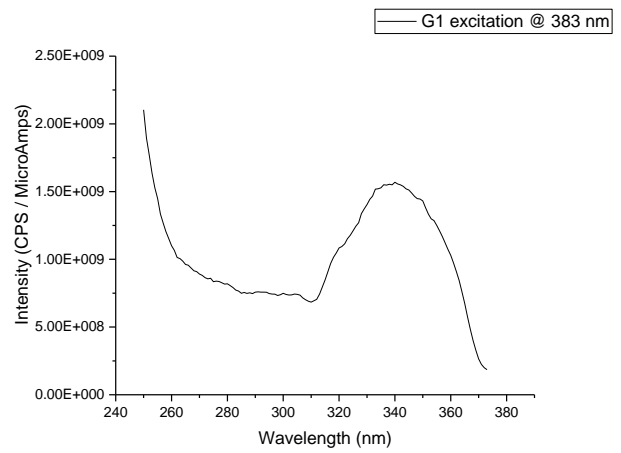
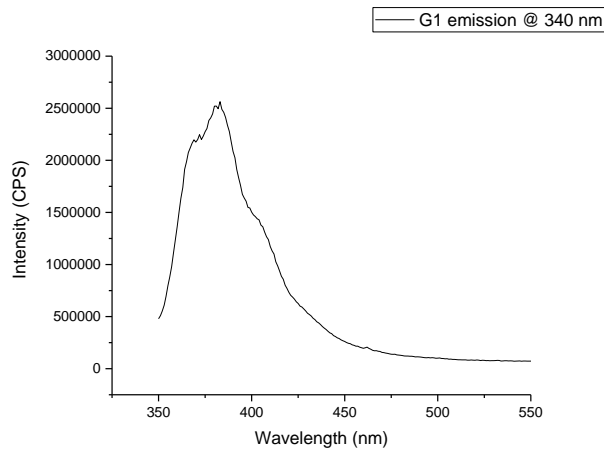
tris(9,9-dimethyl-9H-fluoren-2-yl)(methyl)silane (3):

A 1 liter round bottom flask was charged with 9,9-dimethylfluorene (24.32 g, 89.03 mmol, 3.3 equiv) and THF (180 mL), then cooled to $-78\text{ }^{\circ}\text{C}$. $t\text{BuLi}$ (100 mL of 1.7 M solution in pentane, 169.97 mmol, 6.3 equiv) was added via cannula over the course of 10 minutes. A white precipitate was observed forming in solution. After stirring for 1 hour, MeSiCl_3 (3.17 mL, 26.98 mmol) was added dropwise via syringe. The precipitate dissipated upon addition, yielding a yellow solution. The mixture was allowed to warm to room temperature over the course of an hour and continue to stir overnight. Water (150 mL) was added in one portion and the aqueous phase was extracted with DCM (3 x 60 mL). The combined organics were washed with brine (1 x 50 mL), dried with MgSO_4 , and concentrated *in vacuo* to provide a yellow residue. Purification via flash column chromatography (SiO_2 , 0 to 10% DCM in Hexanes) provided 6.85 g of **3** as colorless crystals (41% yield). ^1H NMR (500 MHz, CDCl_3) δ 7.77 (dd, $J = 2.9, 5.0$, 3H), 7.76 (d, $J = 7.9$, 3H), 7.68, (s, 3H), 7.57 (dd, $J = 0.7, 7.3$, 3H), 7.45 (dd, $J = 2.9, 5.0$, 3H), 7.35 (m, 6H), 1.47 (s, 18H), 0.98 (s, 3H); ^{13}C NMR (125 MHz, CDCl_3) δ 154.0, 153.0, 140.6, 139.2, 135.6, 134.4, 129.5, 127.7, 127.1, 47.0, 27.3, 27.3, -2.2; HRMS (ESI) m/z calcd for $\text{C}_{46}\text{H}_{42}\text{SiNa}$ $[\text{M} + \text{Na}]^+$ 645.2953, found 645.2944.

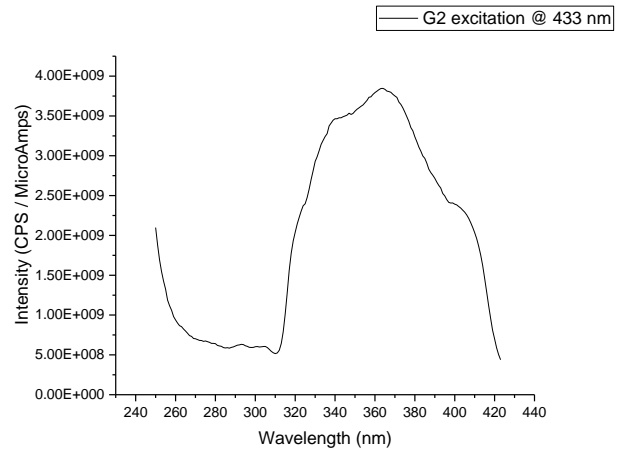
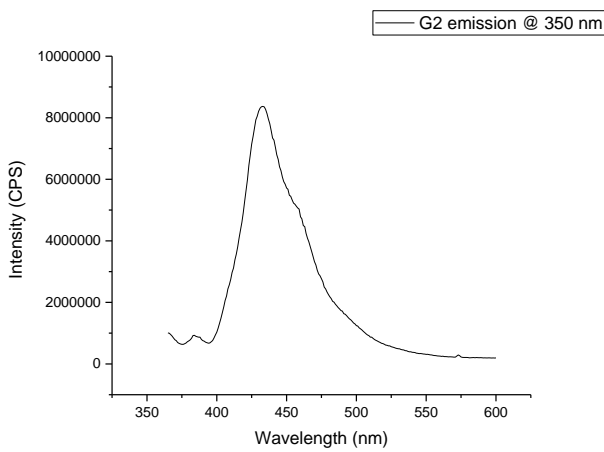
Photoluminescence Spectra for glasses G1 – G6

Quantum Yield measurements were obtained at the absorption maximum. Pictures taken with sample located between two planar polarized filters.

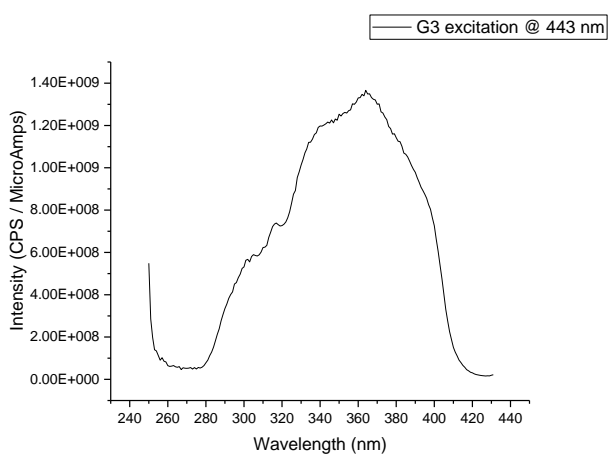
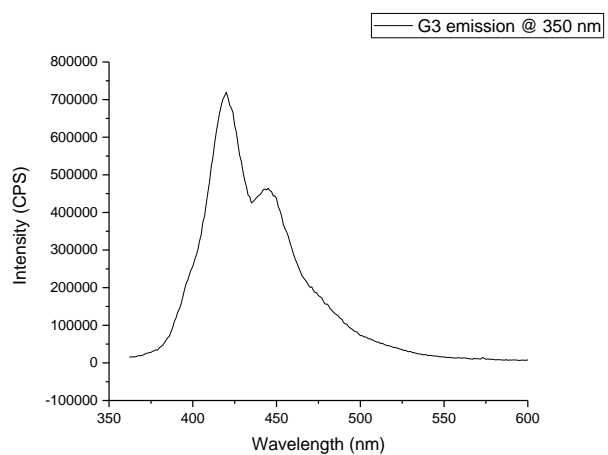
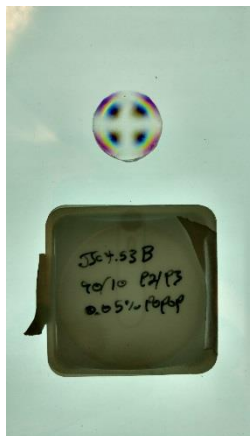
G1; 90/10 1/2



G2; G1 with 0.05% DPA

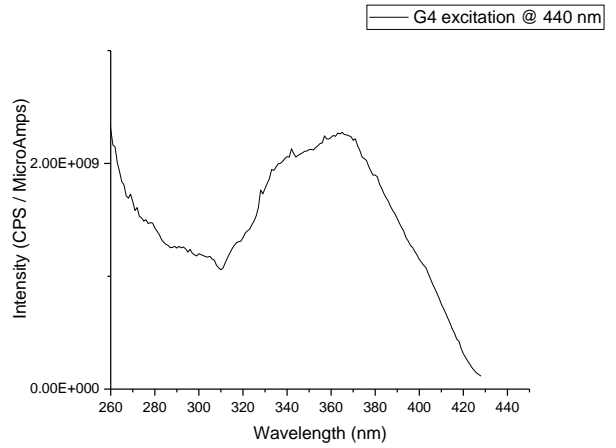
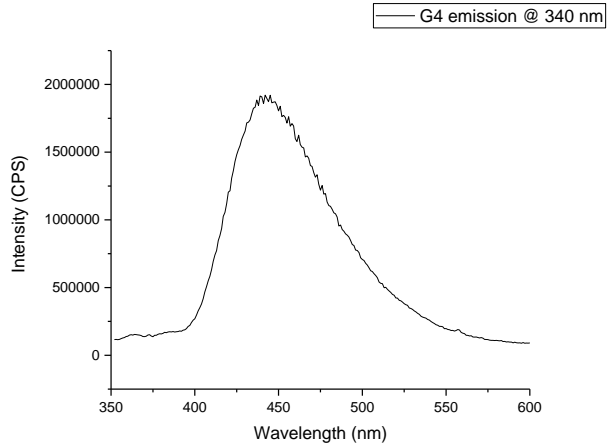


G3; G1 with 0.05% POPOP

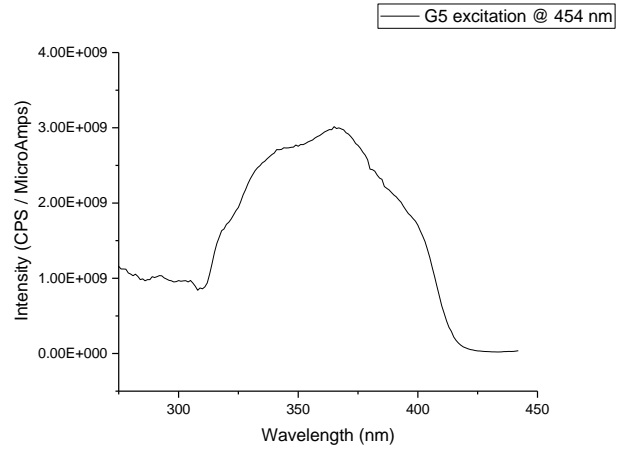
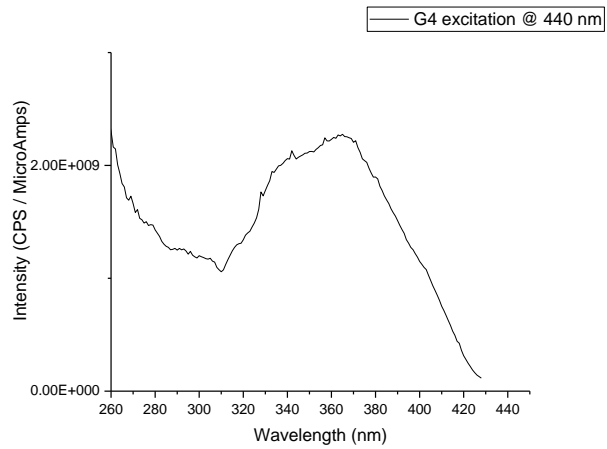


G4; G1 with 0.05% DPVBi

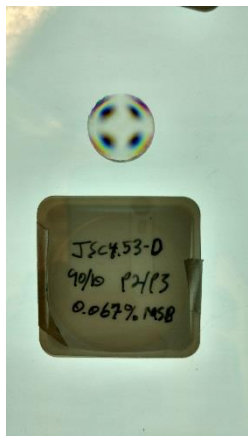


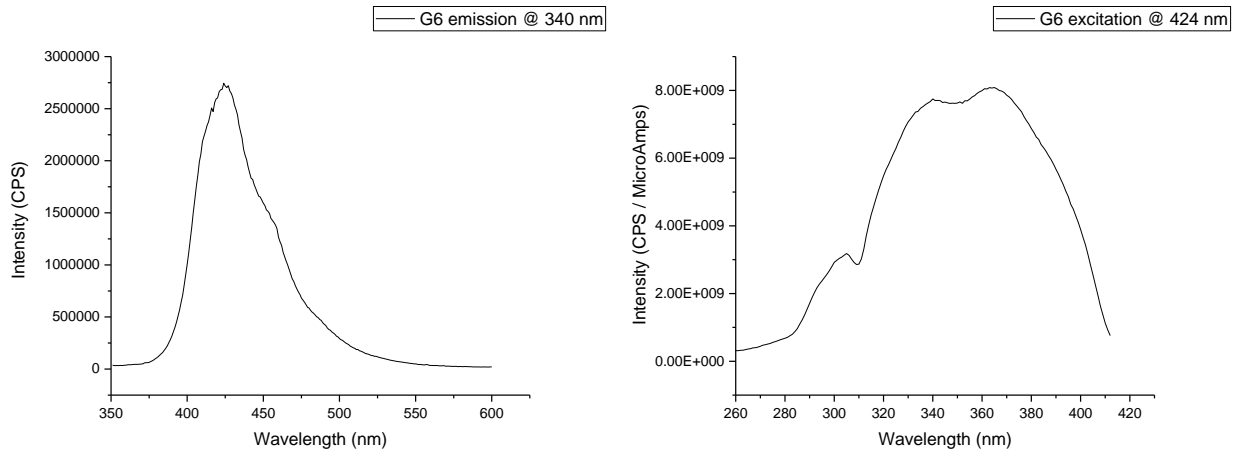


G5; G1 with 0.05% MSB



G6; G1 with 0.07% MSB





Characterization of Radioluminescence

For the reported light yield measurements, the integral of the baseline subtracted pulse from 10 nanoseconds ahead to 170 nanoseconds after the waveform maximum was used as a proxy for total energy deposited. The waveform maximum was determined as the time during the record at which the derivative of the waveform crossed zero; with linear interpolation to provide subsample resolution.

The conversion from this pulse energy to electron equivalent energy (in keVee) was approximated by finding the pulse energy at which the Compton edge reached 70% of the Compton peak value for a ^{137}Cs gamma source measurement.³ We then used 478 keVee/this pulse energy value as a linear conversion to the energy scale.

The pulse shape discrimination parameter used in this work is defined as the time between 10% and 90% of the baseline subtracted pulse integral over the entire waveform record; with linear interpolation to provide subsample resolution. We found that the use of this PSD parameter eliminates the systematic biases that can be introduced by implementing methods that require knowledge of or optimization for the scintillator pulse shape. Because we are

comparing multiple scintillating materials with varying pulse shapes, we did not use more popular methods such as the tail to total ratio so as to not bias their relative performance by any particular time window choice.

In order to characterize the PSD performance of each scintillator, we developed a procedure by which an energy dependent Figure of Merit (FOM) is derived. In this work, we use the familiar FOM definition:

$$FOM(E) = \frac{\mu_n(E) - \mu_\gamma(E)}{(\Gamma_n(E) + \Gamma_\gamma(E))}$$

Where μ stands for the mean of a distribution, Γ stand for the full width at half maximum (FWHM) of a distribution, and the subscripts n and γ refer to the neutron and gamma distributions respectively.

The energy dependent mean and FWHM for the gamma distributions were obtained directly from a gamma-ray “pure” data set taken from measurements of a ^{60}Co radiological source. The means of the PSD distribution were calculated and the FWHMs were obtained by finding the PSD value at which the distribution reached half of the maximum count value above and below of the maximum PSD value for each energy bin (bin width of 17.5 keVee).

Because it is difficult to obtain a neutron “pure” data set, a procedure was developed by which the underlying neutron distribution is estimated from a measurement of a mixed gamma/neutron $^{241}\text{AmBe}$ radiological source. For each energy bin, the PSD distribution from the corresponding bin of the ^{60}Co gamma measurement is scaled and subtracted from the $^{241}\text{AmBe}$ mixed PSD distribution. A scaling factor that minimizes the chi-square on a Gaussian fit to the remaining PSD distribution is selected.

The remaining distribution is used as a neutron “pure” PSD distribution. Although this procedure biases the estimated neutron distribution toward having a Gaussian shape, we have determined that it is more robust to use the actual measured distributions to obtain the means and FWHMs wherever possible rather than relying on fitting double Gaussians to the entire mixed data set. It is often difficult to obtain a reasonable double Gaussian fit, especially in regions in which the gamma and neutron PSD distributions have significant overlap in the low FOM value regions. The mean and FWHM of the Gaussian fit were then used to characterize the neutron distribution for the FOM calculations.

For all light yield, timing, and PSD characterization measurements, the scintillator samples were wrapped in Teflon and coupled with silicone optical grease to an ET Enterprises 9124B bialkali photomultiplier tube (PMT) using a 50 Ω coaxial cable for the readout. The PMT was biased with a Stanford Research Systems (S325/2500-25W) high voltage power supply. Radiological sources were obtained from commercial vendors at the following strengths: ^{137}Cs 8.46 μCu ; ^{60}Co 4.70 μCu ; $^{241}\text{AmBe}$ 29.9 μCu . A single crystal of stilbene ($\frac{3}{4}$ ” diameter cylinder, ca. $\frac{1}{4}$ ” high) was purchased from Inrad Optics and used for all stilbene radioluminescence measurements. EJ-200 and EJ-301 were purchased from Eljen Technology. EJ-200 was machined to 1” diameter cylinders and polished. EJ-301 was bubbled with Argon for 5 minutes to remove oxygen before each radioluminescence measurement.

Characterization of glasses using ezDAQ and SPROCKET

The anode output of the PMT was sampled directly with a CAEN DT5730 14 bit 500 MS/s desktop digitizer with a 2 Volt input full range. A waveform record length of 112 samples with a 20 sample

pre-trigger window was recorded on each self-triggered event. A baseline value was calculated by averaging the first 10 samples in each waveform record.

Characterization of glasses using oscilloscope pulse analysis method

Scintillation pulses were obtained using a 12-bit, 600 MHz LeCroy HRO66Zi oscilloscope to evaluate the relative scintillation light yield for each sample. A 662 keV ^{137}Cs gamma-ray source was used for the energy calibration, which provides a Compton edge energy value of 478 keV. The individual waveforms were digitally integrated in real-time over an interval of 500 ns and histogrammed to obtain the pulse height spectra. The Compton edges were evaluated as the channel number corresponding to 70% of the Compton maximum value.

Scintillation timing measurements

Scintillation timing distributions were obtained for ^{137}Cs γ -rays using the method of time-correlated single-photon counting (TCSPC). A Hamamatsu R1828-01 PMT was used to provide the scintillation trigger pulse, along with an R7207-01 PMT to provide the single-photon stop pulse. The delay times between pulses were histogrammed using a LeCroy HRO66Zi 12-bit oscilloscope to obtain the scintillation decay curves.

Radioluminescence Characterization Figures

In order to obtain average pulse shapes, each waveform's peak time was aligned to zero using the aforementioned derivative zero-crossing method and added with linear interpolation to a separate oversampled summed waveform (with 100 picosecond resolution) for each energy bin. The oversampled summed waveform was then divided by the total number of contributing waveforms.

The average gamma-ray pulse shape was obtained using the ^{60}Co measurement while the average neutron pulse shape was obtained from the $^{241}\text{AmBe}$ measurement for only those waveforms whose PSD value was greater than a threshold value. The threshold value for each energy bin was determined as the PSD value at which only 1% of the events in the ^{60}Co measurement have a larger PSD value (Figure 8).

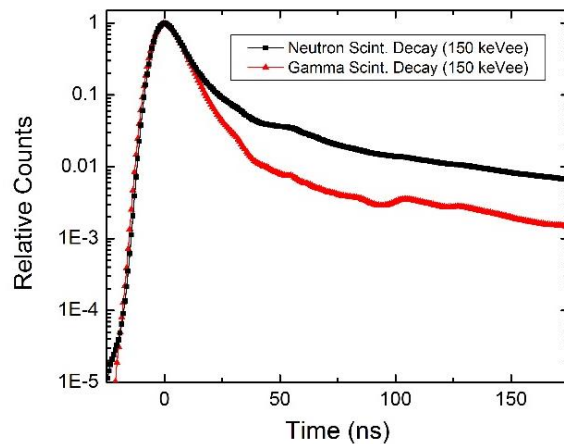


Figure S2. Average scintillation pulse shapes obtained for 150 keV neutrons (black) and gamma-rays (red) in **G5** glass.

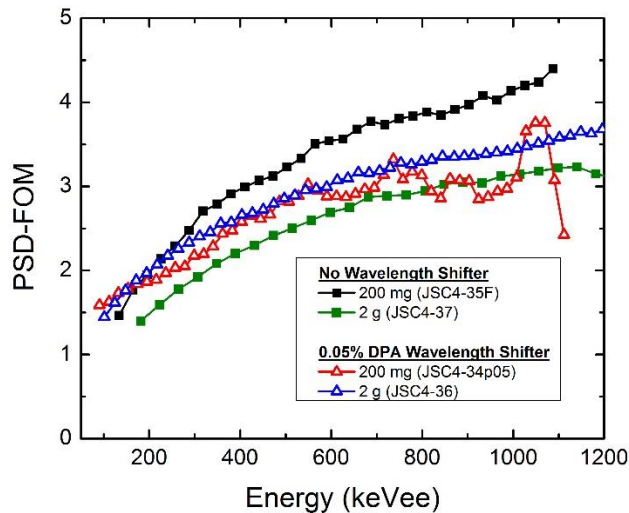


Figure S3. Size dependence on PSD performance. Performance drop is more pronounced in sample with no wavelength shifter due to self-absorption.

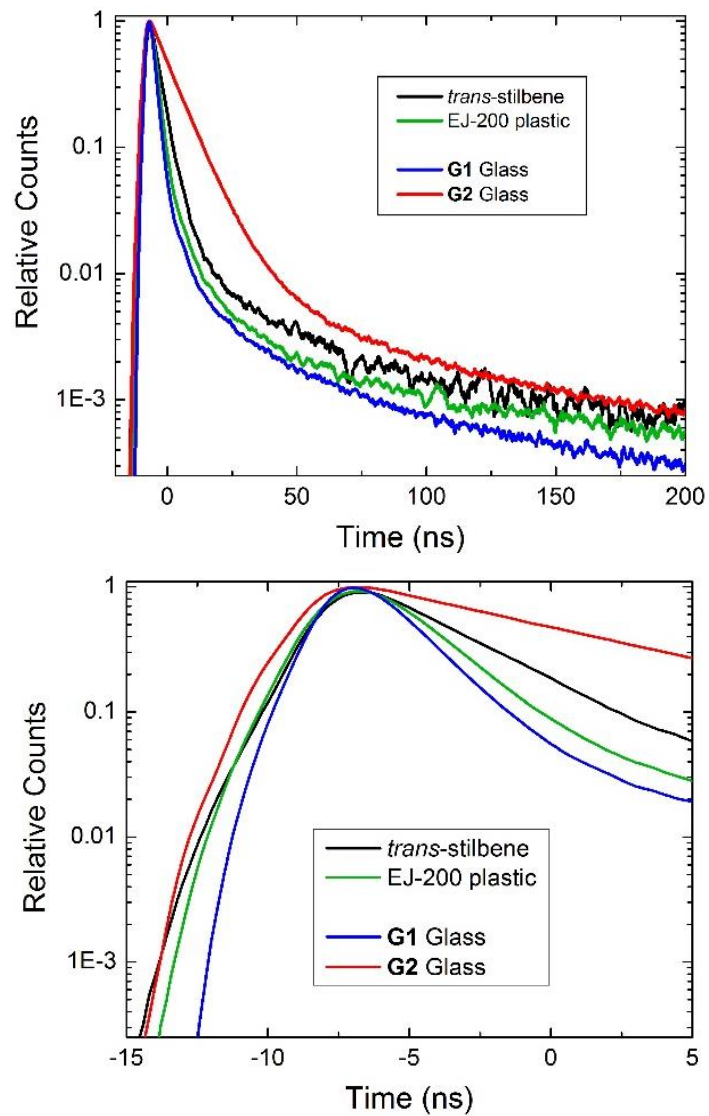


Figure S4. Normalized scintillation timing via time correlated single-photon counting in the presence of a ^{137}Cs source (top), zoomed in region at the pulse max amplitude (bottom).

DSC Spectra

Differential scanning calorimetry (DSC) measurements were taken using a Mettler Toledo DSC822 instrument and evaluated using STARe software; values for T_g are reported at the onset of the transition. Runs were performed with no blank subtraction, under a stream of Argon (10 ml/min) with the following profile:

-20 °C to 300 °C @ 10 °C/min

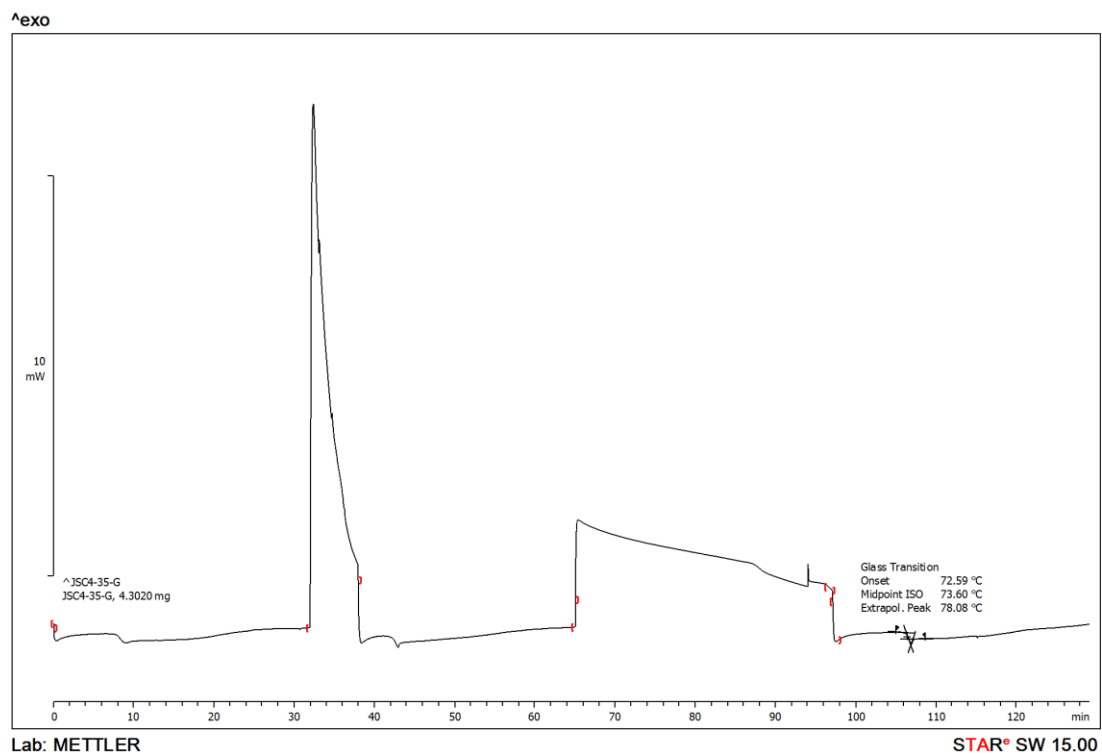
300 °C to -20 °C @ 300 °C/min (quench cool)

-20 °C to 300 °C @ 10 °C/min

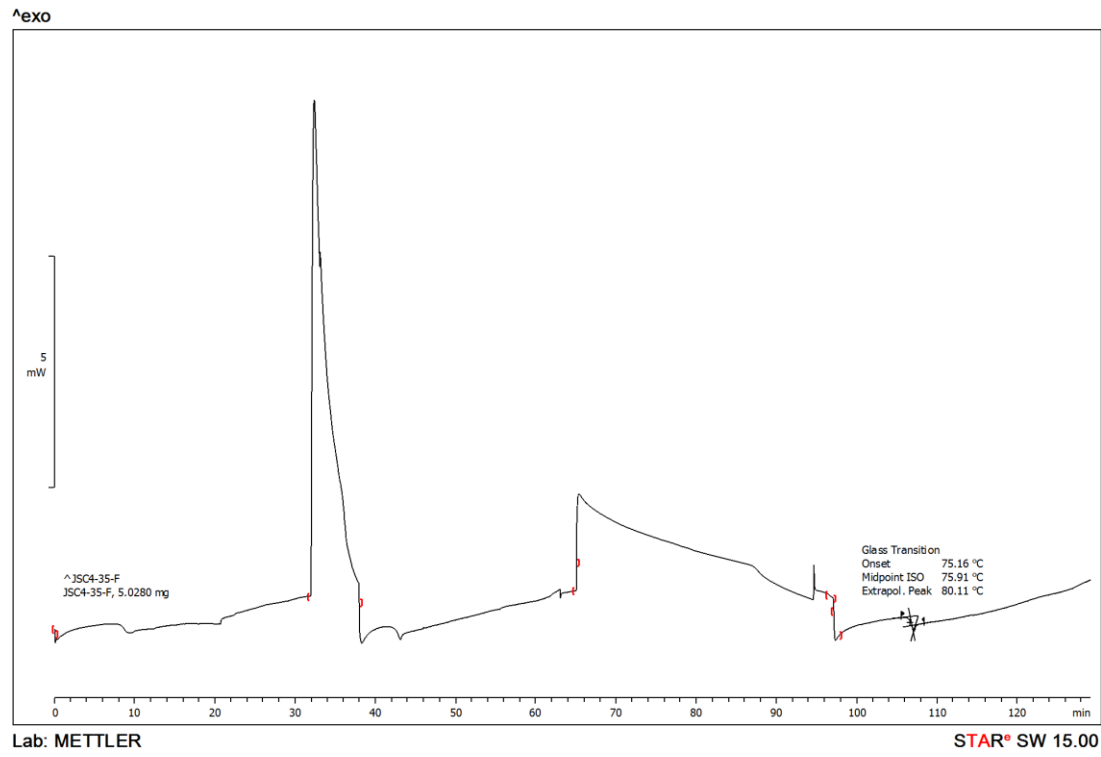
300 °C to -20 °C @ 10 °C/min

-20 °C to 300 °C @ 10 °C/min

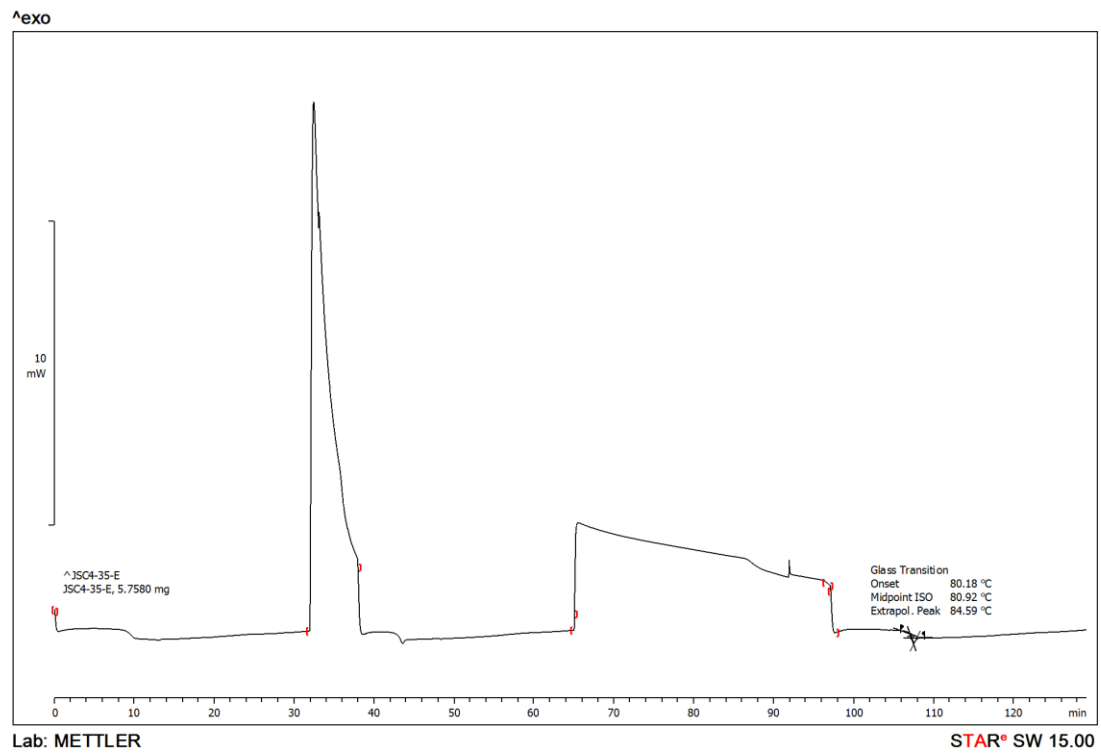
Compound 1



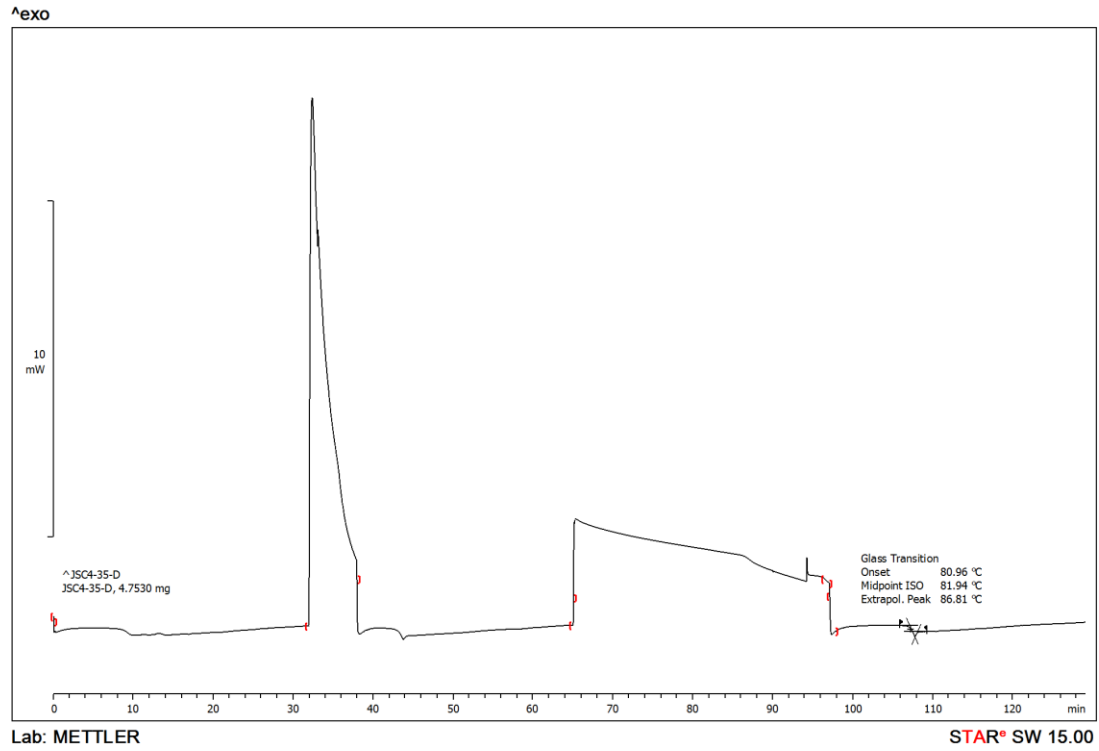
90 : 10 (w/w) 1:2



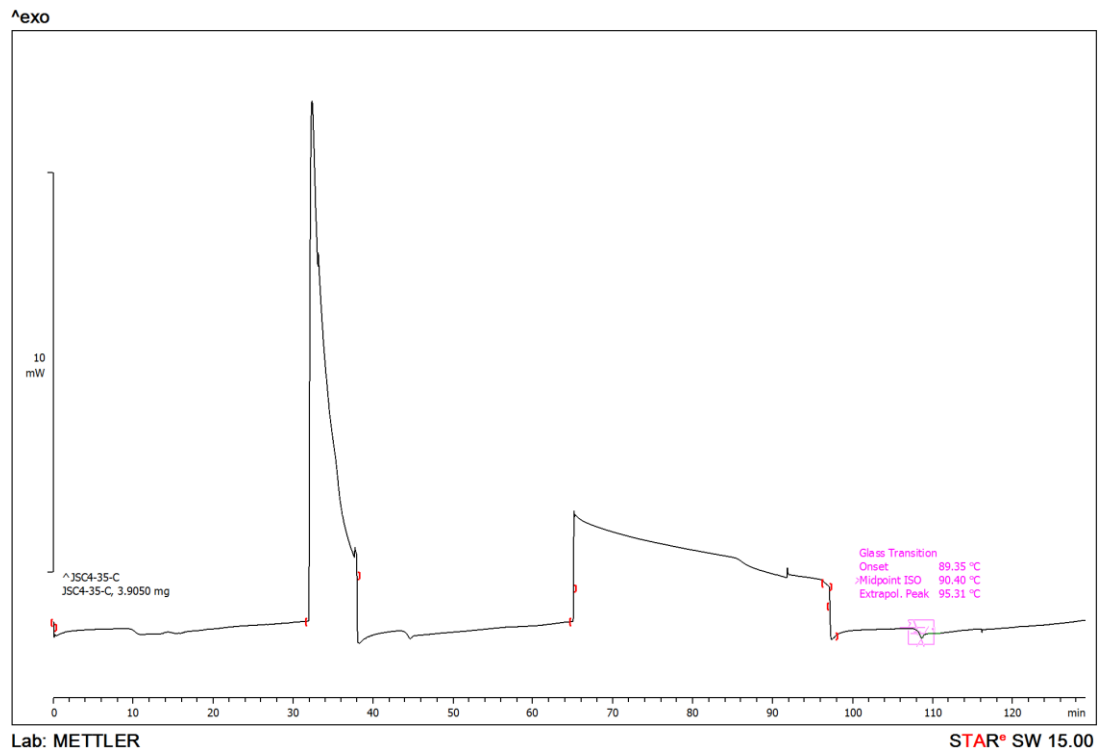
70 : 30 (w/w) 1:2



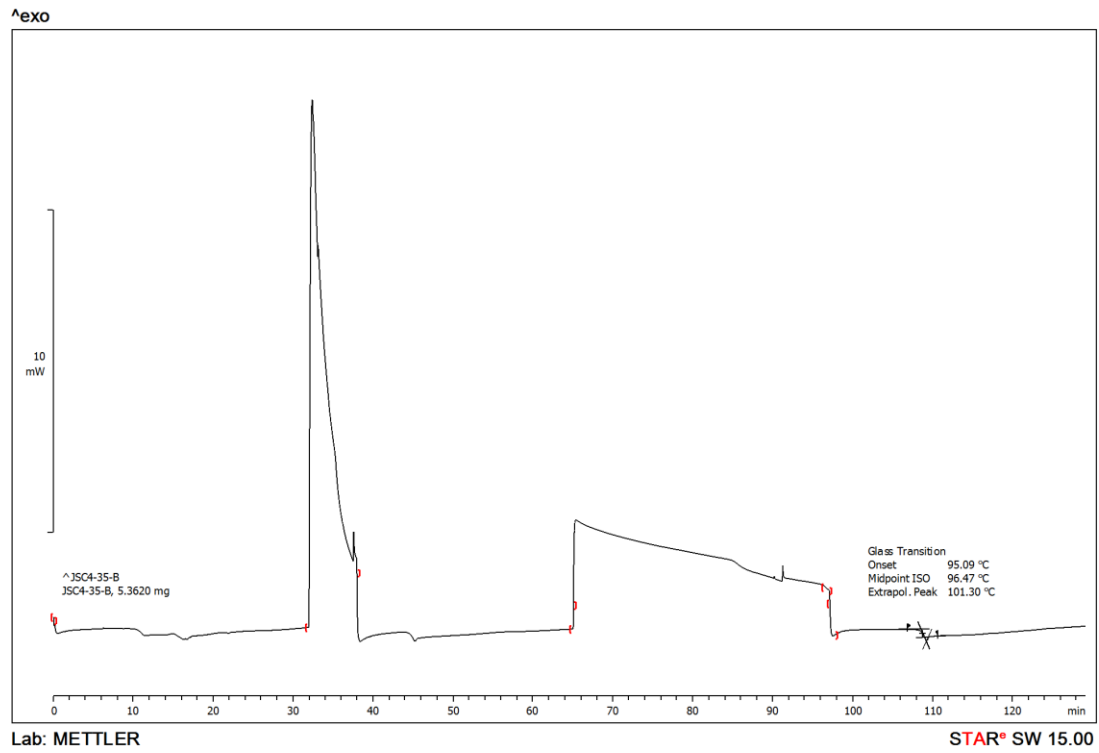
50 : 50 (w/w) 1:2



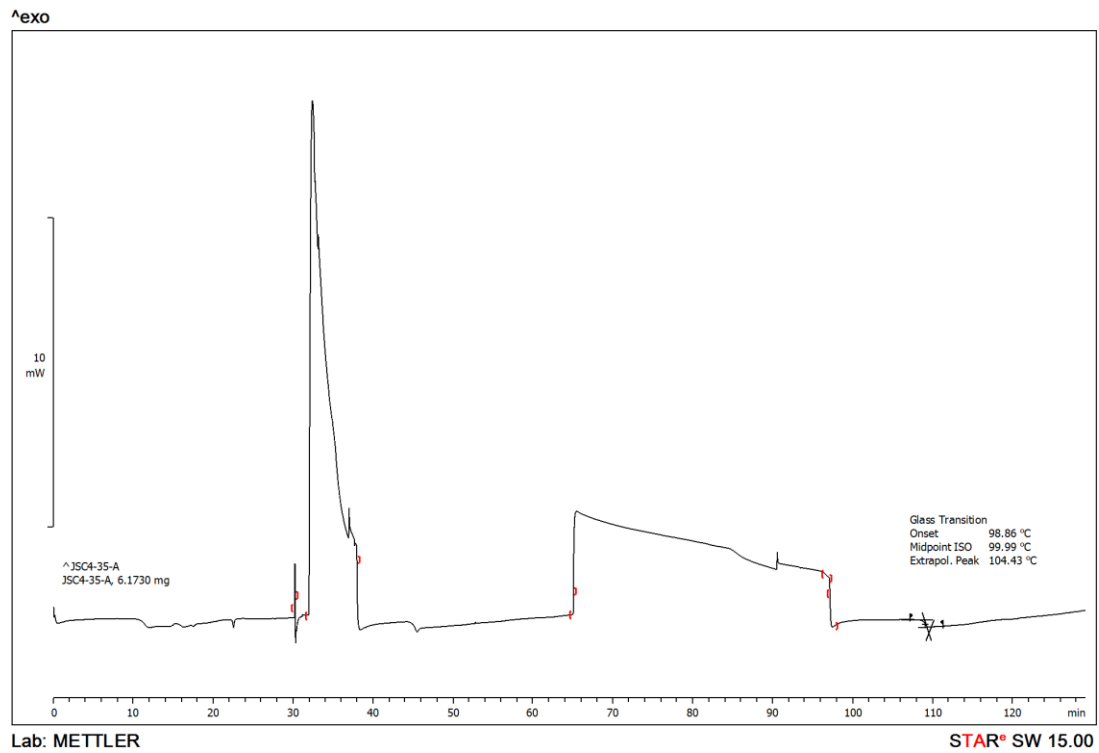
30 : 70 (w/w) 1:2



10 : 90 (w/w) 1:2

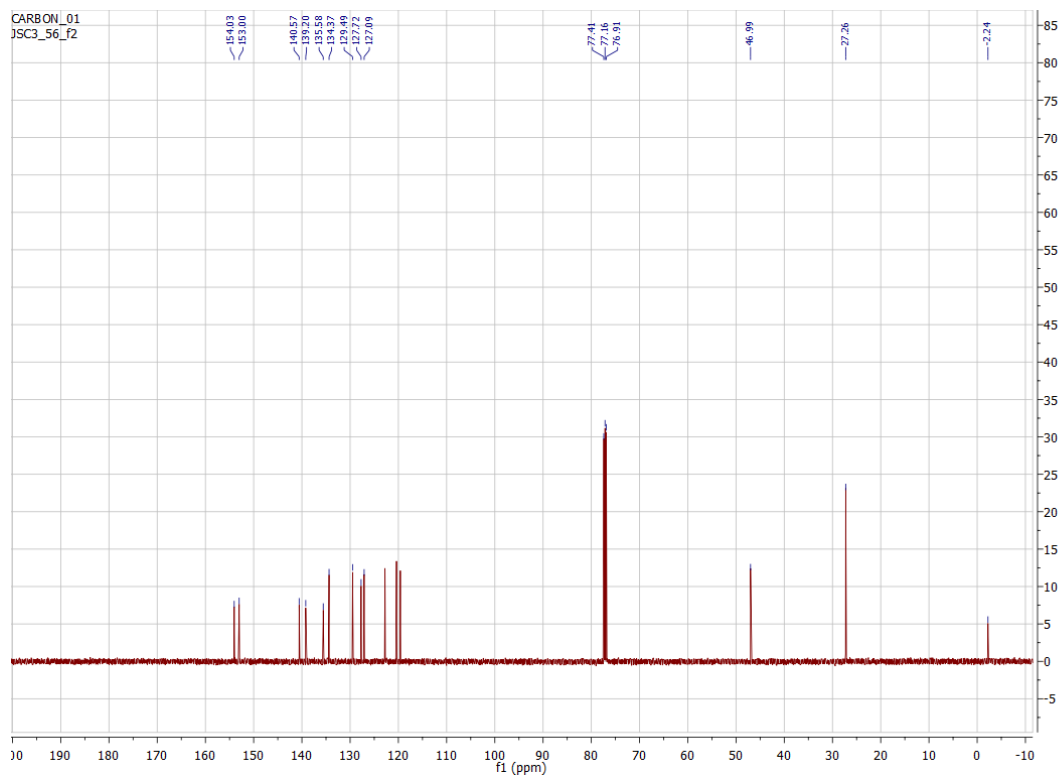
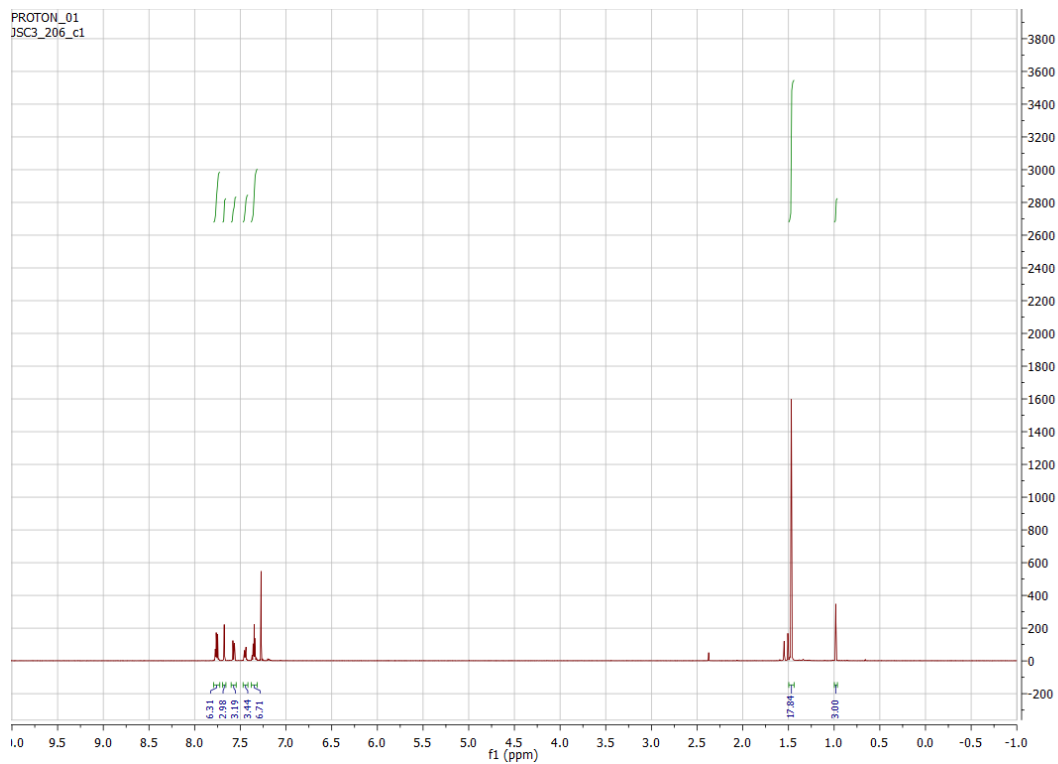


Compound 2



NMR Spectra

Compound 3



Powder X-ray Diffraction Experimental

Powder X-ray diffraction experiments were performed on an Empyrean PANalytical X-ray with a ω - χ -spinner sample stage, taken from 2-75 Θ in 0.026 Θ steps at 36.465 seconds per step.

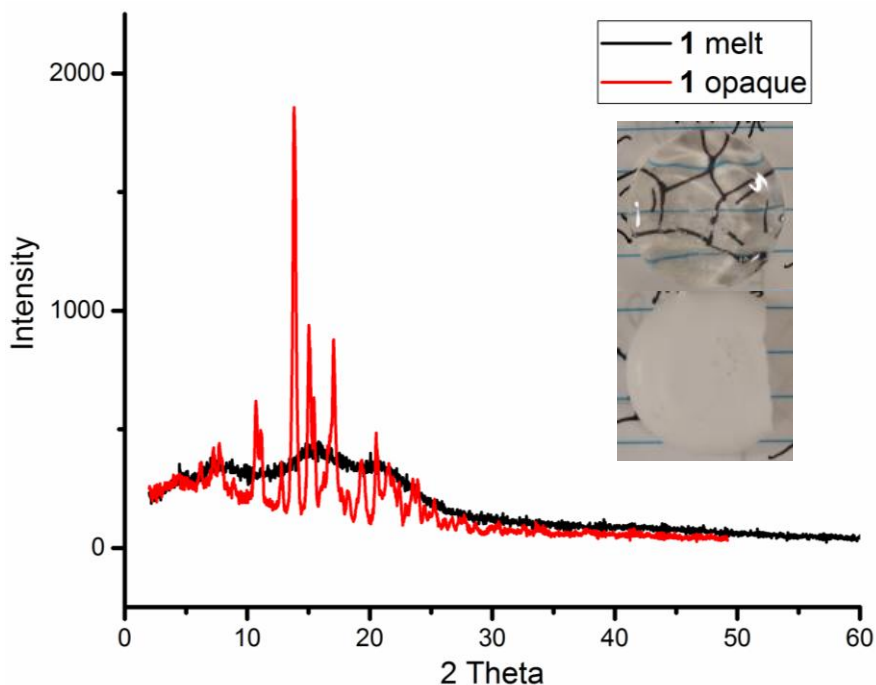


Figure S5. Powder XRD of **1** depicting the change from clear and amorphous 2 gram sample to opaque and crystalline over time.

References

- ¹ Carman, L.; Zaitseva, N.; Martinez, H. P.; Rupert, B.; Pawelczak, I.; Glenn, A.; Mulcahy, H.; Leif, R.; Lewis, K.; Payne, S. *J. Cryst. Growth* **2013**, *368*, 56–61.
- ² Wei, W.; Djurovich, P. I.; Thompson, M. E. *Chem. Mater.* **2010**, *22*, 1724–1731.
- ³ The approximation of the Compton edge at 70% of the peak is a close approximation of the correct energy scale, and typical for organic scintillators: Dietze, G.; Klein, H. *Nucl. Instrum. Methods* **1982**, *193*, 549–556.